Membranes

Deutsche Ausgabe: DOI: 10.1002/ange.201603644
Internationale Ausgabe: DOI: 10.1002/anie.201603644

Synthesis of Discrete Alkyl-Silica Hybrid Nanowires and Their Assembly into Nanostructured Superhydrophobic Membranes

*Deliang Yi, Chenglong Xu, Ruidie Tang, Xuehua Zhang, Frank Caruso, and Yajun Wang**

Abstract: *We report the synthesis of highly flexible and mechanically robust hybrid silica nanowires (NWs) which can be used as novel building blocks to construct superhydrophobic functional materials with three-dimensional macroporous networks. The hybrid silica NWs, with an average diameter of 80 nm and tunable length of up to 12 μm, are prepared by anisotropic deposition of the hydrolyzed tetraethylorthosilicate in water/n-pentanol emulsions. A mechanistic investigation reveals that the trimethoxy(octadecyl)silane introduced to the water-oil interface in the synthesis plays key roles in stabilizing the water droplets to sub-100 nm and also growing a layer of octadecyl groups on the NW surface. This work opens a solution-based route for the one-pot preparation of monodisperse, hydrophobic silica NWs and represents an important step toward the bottom-up construction of 3D superhydrophobic materials and macroporous membranes.*

Nanostructured silica materials have been widely used as substrates or templates for the preparation of functional materials because of their high specific surface area, tunable porosity and morphology, high biocompatibility, good chemical and thermal stability, and facile surface modification by silane chemistry.[1–4] For example, silica particles with uniform spherical morphology have been used as building blocks to construct colloidal crystals[2] and supraparticles,[3] and higher-order particle-assembled structures have been used as templates to prepare inverse opals or three-dimensionally ordered macroporous (3DOM) materials.[4]

Recently, high aspect ratio particles (e.g., carbon nanotubes, metal, and metal oxide nanowires) have been employed as building blocks to prepare nanowire (NW) membranes with diverse functionalities (e.g., catalysis, sensing, and molecular separation).[5] However, to the best of our knowledge, NW membranes based on the assembly of silica NWs has not been reported. This absence in the literature is probably because of the challenges associated with synthesizing high quality silica NWs, which are required as the building blocks. Although silica particles with high aspect ratios have been prepared by various synthetic techniques, such as vapor-liquid-solid deposition,[6] casting,[7] flame-brushing,[8] electrospinning,[9] and sol-gel template synthesis,[10] these methods usually require special equipment, can be difficult to scale up, or do not provide well-dispersed particles in solution. Therefore, developing a robust technique that is capable of producing discrete, high quality silica NWs which can be used as building blocks is of particular importance, both for fundamental studies and technological applications.

Herein, we report the preparation of discrete silica NWs with a hydrophobic surface by anisotropic sol-gel growth in a water/oil emulsion. Alkyl-capped silica NWs, with a diameter of approximately 80 nm and tunable aspect ratios (1–150), are obtained using a one-pot wet chemistry synthetic approach. The prepared hybrid silica NWs are mechanically robust and flexible, thus enabling them to be used as building blocks in assembling novel three-dimensional (3D) materials, such as superhydrophobic NW coatings, self-supported NW membranes, and NW monoliths. Superhydrophobic surfaces, with a water-contact angle (CA) higher than 150°, have attracted attention in both fundamental research and practical applications ranging from anti-fouling, self-cleaning, and oil/water separation to microfluidic devices.[11–16] Compared with various other techniques such as lithography,[12] electrospinning,[13] chemical vapor deposition,[14] electroless galvanic deposition,[15] anodic oxidation, and electrochemical deposition[16] used to create a superhydrophobic surface, the bottom-up construction of a 3D superhydrophobic surface by the assembly of lipophilic silica NWs is simple, inexpensive, and requires no special equipment or chemical post-treatment.

The synthesis of silica NWs is inspired by the work of Kuijk et al.,[17] who introduced the preparation of rod-like silica colloids with a diameter of 200–300 nm by an anisotropic growth method in water/*n*-pentanol emulsions. The present work, however, led to a new concept to prepare ultrathin silica NWs through introducing the surfactant-like hydrolysate of trimethoxy(octadecyl)silane (C_{18}TMOS) to the water–oil interface to stabilize the water droplets to sub-100 nm. Meanwhile, a layer of octadecyl (C_{18}) groups is simultaneously grown on the NW surface to endow it with hydrophobicity (Figure 1 g), which allows good dispersion of the high aspect ratio NWs in the organic synthesis solvent (*n*-pentanol).

[*] Dr. D. L. Yi, R. D. Tang, Prof. Y. J. Wang
Department of Chemistry, Fudan University
Shanghai 200433 (P.R. China)
E-mail: yajunwang@fudan.edu.cn
C. L. Xu
Department of Chemical and Biomolecular Engineering
The University of Melbourne
Parkville, Victoria 3010 (Australia)
Prof. F. Caruso
ARC Centre of Excellence in Convergent Bio-Nano Science and Technology, and the Department of Chemical and Biomolecular Engineering, The University of Melbourne
Parkville, Victoria 3010 (Australia)
Assoc. Prof. X. H. Zhang
School of Engineering, RMIT University
Victoria 3001 (Australia)
Supporting information and the ORCID identification number(s) for the author(s) of this article can be found under http://dx.doi.org/10.1002/anie.201603644.

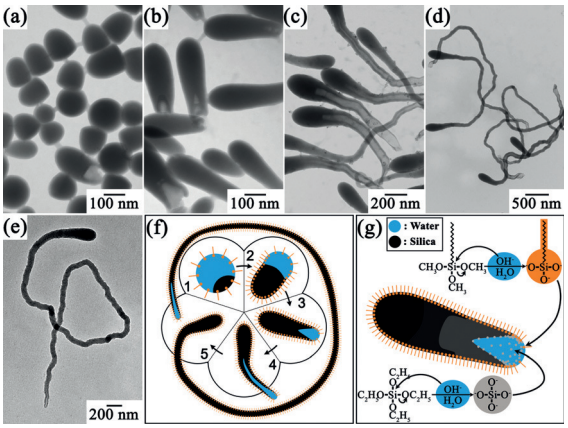

Figure 1. TEM images of bullet-like silica particles (a), fish-like silica nanorods (b), tadpole-like silica nanotubes (c), and snake-like silica nanowires with a length of ca. 4 μm (d) and 7 μm (e) after a growth time of 0.5 h, 1 h, 2 h, 4 h, and 8 h, respectively. f,g) Postulated growth mechanism of the silica nanowires. f(1): nucleation of silica nanoparticle in a water droplet through the condensation of hydrolyzed TEOS, which was transferred into a water droplet from the oil phase, f(2): formation of bullet-like silica nanoparticle by anisotropic condensation of the hydrolyzed TEOS inside the water droplet, f(3): fishlike silica nanorod formed because of a decrease in the diameter of the water droplets mediated by C_{18}TMOS, f(4): C_{18}TMOS-mediated formation of a silica nanotube, f(5): the further growth of the silica nanotube into a nanowire. g) An enlargement of [f(3)] to illustrate the possible mechanism of elongating the water droplet to form a nanotube structure. The blue regions in (f) and (g) represent the water phase and the gray regions represent the sol-gel growth of silica.

Evolution of the silica NWs is studied through tracking morphology variations of the intermediate products by transmission electron microscopy (TEM).A postulated growth mechanism is illustrated in Figure 1 f. Silica nanoparticles with a bullet-like shape (Figure 1 a) are nucleated within 30 minutes because of the anisotropic deposition of hydrolyzed TEOS inside the water droplet at basic pH conditions (Figure 1 f(1)), as reported in previous literature.[17] To reduce its surface energy, the nucleated silica nanoparticles deposit at the interface of the droplets, thus resulting in anisotropic droplets. As one side of the silica nanoparticle is contacted with the oil phase, the sol-gel growth of the silica can only occur in the opposite direction (i.e., in the water phase of the droplet). Sodium citrate in the water droplets has the function of stabilizing the hydrolyzed TEOS, and transporting it to the existing nucleus in the droplet (see Figure S1). Meanwhile, the C_{18}TMOS dissolved in the oil phase (*n*-pentanol) hydrolyzes into $C_{18}Si(O^-)_3$ when it encounters basic water droplets. Importantly, the $C_{18}Si(O^-)_3$ possesses amphiphilic properties and thus arranges on the droplet surface with its hydrophilic $Si(O^-)_3$ ion facing the water phase, and the C_{18} tail facing the *n*-pentanol solvent (Figure 1 f(2)). Playing a similar role to a surfactant, the interfacially arranged $C_{18}Si(O^-)_3$ reduces the surface tension of the water droplet, which is attached to the nucleated silica nanoparticle. Under lower surface tension, the initial water droplet is deformed into a more elongated cone-like structure (Figure 1 f(3) and 1 g), and then forms a tadpole-like silica nanorod as particle growth progresses (Figure 1 c). With the continuous hydrolysis/condensation reaction of TEOS (Figure 1 f(4 and 5)), a silica NW is eventually developed (Figure 1 d), and grows to its full length when the added TEOS is consumed.

The fully grown silica NW has a diameter of approximately 80 nm (Figure 2 a), and resembles a snake-like shape with a short head and slim body, whose aspect ratio can reach as high as 150 (Figure 2 b). The silica NWs remain intact (Figure 2 c) after 1 hour of vigorous sonication (50 kHz, 240 W) in water, thus demonstrating high flexibility and mechanical robustness of the NWs. The curly shape of the NWs observed in the TEM image is likely caused by the lipophilic interaction of the NW when it is vigorously sonicated in water solution. The hybrid silica NW has a Young's modulus of about 14.4 ± 2.5 GPa (see Figure S2 in the Supporting Information), as measured with an atomic force microscope (AFM) using a similar method reported earlier.[18] This value is approximately two-fold higher than the Young's modulus obtained from the calcined silica NW (ca. 7.1 ± 2.1 GPa), which agrees with previous reports that hybrid materials can exhibit enhanced mechanical properties

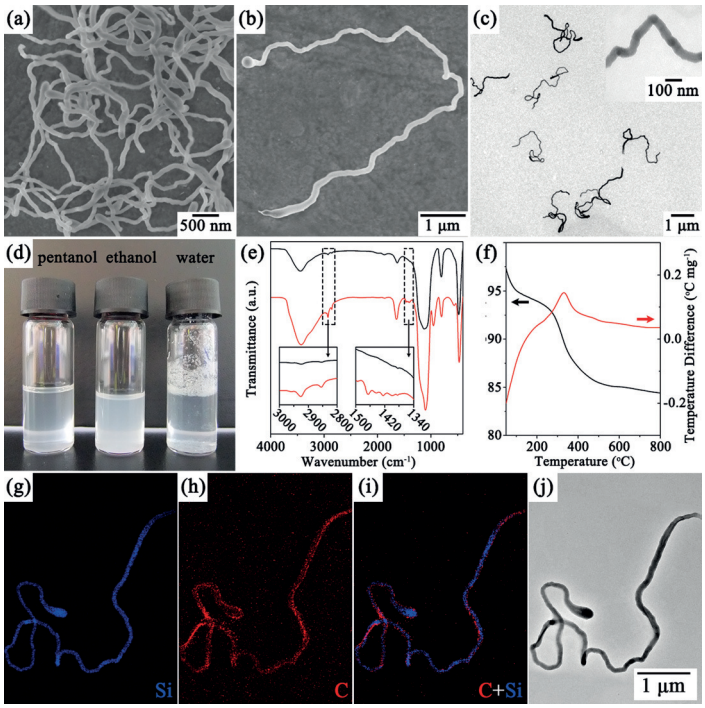

Figure 2. SEM images of silica NWs after drying from concentrated (a) and highly diluted (b) colloidal solutions. c) TEM image of silica NWs after 1 h of vigorous sonication in water. The inset is a higher magnification of a NW. d) Digital photographs of the as-prepared silica NWs dispersed in pentanol, ethanol, and water, respectively. e) FTIR spectra of the as-prepared (bottom) and calcined (top, calcined at 550 °C for 3 h) silica NWs. f) Thermogravimetry/differential thermal analysis plots of the as-prepared silica NWs. Elemental mapping profiles of Si (g) and C (h), and a color-merged image (i) in the silica NW shown in (j).

because of the interfacial bonding between organic and inorganic phases.[19]

The hybrid silica NWs can be well dispersed in alcohol (e.g., ethanol, propanol, and pentanol), thus forming stable colloidal solutions without apparent sediments for up to two weeks (Figure 2d). However, foam-like flocculation is formed once the NWs are transferred into water (Figure 2d), and highlights the hydrophobic properties of the silica NWs. This feature is a result of the silica NWs being capped with a layer of C_{18} alkyl groups, as corroborated by the Fourier transform infrared (FTIR) spectra (Figure 2e). The peaks at 2850 cm^{-1} and 2925 cm^{-1} in the spectra of the as-synthesized silica NWs are symmetric and asymmetric stretching vibrations, respectively, of -CH_2- while the peaks at 1465 cm^{-1} and 1380 cm^{-1} can be ascribed to the symmetric bending vibrations of -CH_2- and -CH_3, respectively. The strong band at 1100 cm^{-1} can be assigned to the asymmetric stretching vibration of Si-O-Si, and the peaks at 470 cm^{-1} and 800 cm^{-1} correspond to the symmetric stretching and deformation modes of Si-O-Si.[20] Thermogravimetric analysis yields a quantitative organic content of about 9 wt% in the hybrid silica NWs, which is determined from the weight loss of the hybrid NWs within the temperature range of 200–450 °C. This value is close to the 8.6 wt% (compared with TEOS) of C_{18}TMOS added in the NW synthesis. Notably, the C_{18} alkyl groups are distributed across the whole length of the NWs, as revealed from the carbon elemental mapping profiles shown in Figure 2g–i.

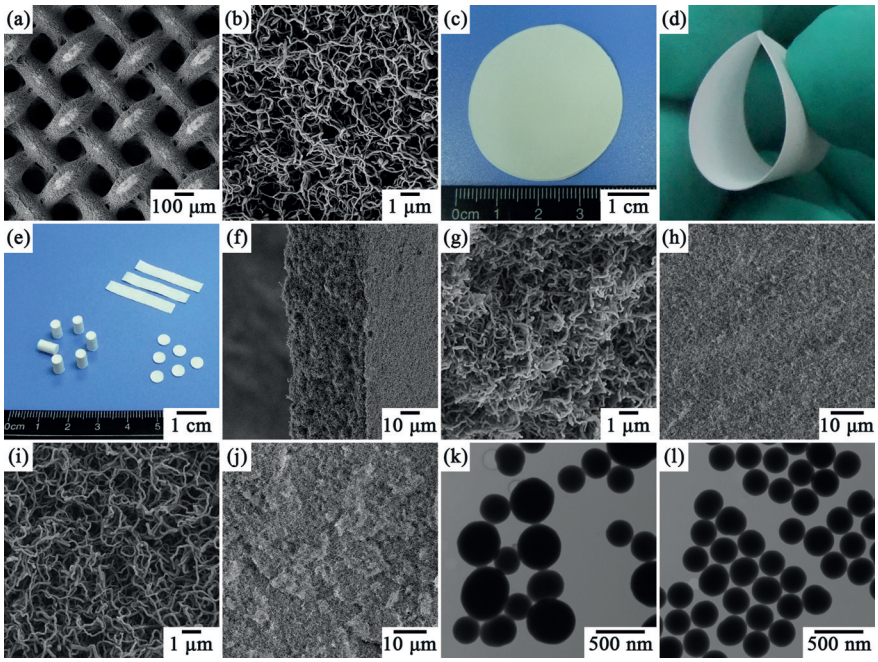

Figure 3. SEM images of a stainless steel wire mesh coated with silica NWs at low (a) and high (b) magnifications. Digital photographs of a free-standing silica NW membrane obtained after peeling the NW membrane from the substrate (c) and the NW membrane after bending (d). e) Digital photographs of NW membranes and/or monoliths with different shapes. SEM images of the cross-section (f,g) and outer surface (h,i) of the silica NW membrane shown in (c), at different magnifications. j) SEM image of the silica NW membrane after polishing with a 600 grit sand paper to reveal the structures inside the membrane. The films, membranes and monoliths were prepared from NWs with a growth time of 24 h. TEM images of mixed silica nanoparticles from two sizes of particles (k) and the nanoparticles which have filtrated through the NW membrane (l).

Because of their monodispersity and colloidal stability in solvent, hybrid silica NWs meet the key criteria for use as building blocks. When a liquid film made of the NW colloidal solution is dip-coated on a substrate (e.g., stainless steel wire mesh, glass slide or silicon wafer), the NWs will be driven to the substrate under capillary force action during the drying process, thereby forming a porous NW film which is tightly attached to the substrate (Figure 3a). High magnification SEM images reveal that the silica NWs are self-woven into a porous network (Figure 3b; see Figure S3). The adhesive property of the hybrid NWs is primarily attributed to their high aspect ratio and flexibility, which enables the NWs to form a 3D network over the substrate. Furthermore, the hydrophobic interaction among the C_{18} alkyl groups capped on the silica NW could enhance the adhesion of the assembled NW networks, which mimics gecko-inspired fibrillar adhesives as lipids are also found in the gecko setae surface.[21]

Free-standing silica NW membranes can be assembled by a vacuum filtration method (see Figure S4), which has been used in assembling membranes composed of other NWs.[5a] The diameter of the silica NW membranes is determined by the size of the suction funnel, while the thickness of the membranes can be adjusted through changing the amount of NWs used in membrane assembly. It is noted that multiple silica NW membranes or monoliths with various morphologies (Figure 3e) can be produced in one preparation by mounting a multihole plate inside the funnel (see Figure S5).

A filter-paper-like silica NW membrane with a diameter of 4 cm and thickness of 40 μm is shown in Figure 3c. The silica NW membrane has high flexibility, and can endure bending multiple times without apparent damage (Figure 3d). This membrane possesses a tensile strength of (7.21 ± 0.73) MPa, thus demonstrating its high mechanical robustness. SEM images taken from both the membrane cross-section (Figure 3f,g) and surface (Figure 3h,i) reveal that the NW membrane has a network architecture formed by NWs in 3D. Notably, the NW networks lead to homogeneously distributed structural macropores across the membrane, as seen from high-resolution SEM images (Figure 3g,i). Although it is difficult to observe the individual NWs, no apparent breakage of the NWs can be observed from the cross-section (Figure 3g). Further, the assembled NW membrane can be disassembled in organic solvent (e.g., ethanol, pentanol) under sonication without breaking the NWs, thus demonstrating the robustness and flexibility of the hybrid silica NWs. The NW membrane has a low bulk density of

about 0.3 g cm^{-3} and a high porosity of about 80 % measured by Archimedes' method. The permeability of the macropores inside the membrane was also investigated by filtering colloidal particles of two different sizes (300 and 500 nm; Figure 3 k) through the NW membrane (see Figure S6). The separation result shows that only the 300 nm silica nanoparticles can penetrate through the membrane (Figure 3 l), thus indicating the macropores in the NW membrane are relatively uniform.

The wettability of the NW membrane was studied by measuring the water contact angles (CA) of the surface. The NW membrane has a static water CA of about 162° (Figure 4 a; see Movie S1) and a water sliding angle of less than 1° (Figure 4 b; see Movie S2), thus revealing a superhydrophobic surface. The superhydrophobicity of the membrane is primarily attributed to the C_{18} alkyl groups covering the silica NW building blocks. After removal of the C_{18} alkyl groups (by calcination), water droplets applied on the NW membrane surface are quickly spread and infiltrated into the membrane (Movie S3). Furthermore, the hierarchical network in the membrane also contributes significantly to the superhydrophobicity. In a control experiment, the smooth surface of a glass slide after C_{18}TMOS modification has a significantly lower water CA of about 118° (see Figure S7). The networks with an ultrafine NW diameter (ca. 80 nm) and high surface area (70 m^2 g^{-1}, BET method) have built a high-energy barrier for water droplets to create a liquid–solid interface on the surface. Additionally, the abundant macropores in the NW networks can trap air inside, which provides an air cushion on which to suspend the water droplets.[22]

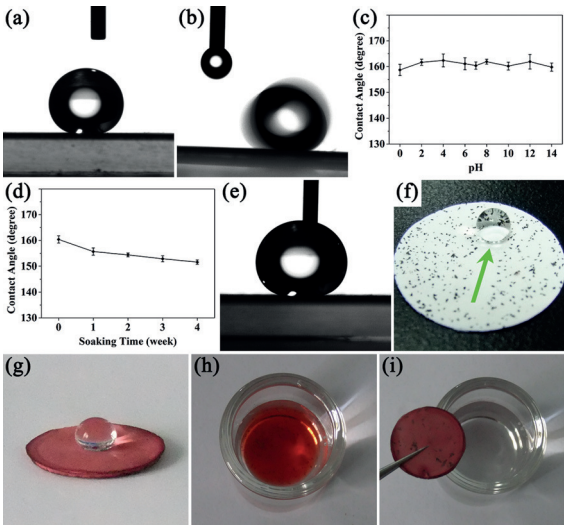

Figure 4. Shape of water droplet on the silica NW membrane (a), and rolling of water droplet on the membrane with a sliding angle of 1° (b). Variation of water CA on the silica NW membrane at different pH values (c) and after immersing the membrane in water for different periods of time (d). e) Shape of the water droplet on the silica NW membrane polished with fine sand paper (600 mesh) to remove the outer layers. f) Digital photographs of cleaning graphite scraps on the membrane with a rolling water droplet (the green arrow indicates the motion path of the water droplet). g) Photo of a silica NW membrane after a drop (500 μL) of water and hexane (colored with Oil Red O) mixture was applied on the surface. Digital photographs of hexane (colored with Oil Red O) contaminated water (h), and the water after the contaminated hexane was removed by the NW membrane (i).

The water CAs on the NW membrane are almost identical (~160°) across a wide pH range, that is, from 0 to 14 (Figure 4 c). The stability of the NW membrane under water was also investigated through immersing the membrane in a water bath for different times. The water CAs slightly decrease as the soaking time increases (Figure 4 d), but the superhydrophobicity of the membrane is still maintained (CA, ca. 152°) after being immersed in water for four weeks. This duration demonstrates that the C_{18} alkyl groups on the silica NW surface can effectively maintain the superhydrophobic properties of the membrane in a wet environment. Of particular significance is that the NW membrane displays superhydrophobicity across its entire thickness as the whole membrane is assembled of lipophilic NWs. To investigate the membrane internal properties, the NW membrane was polished with fine sand paper to remove the outer NW layers. Interestingly, the water CA on the polished membrane increased slightly to about 164° (Figure 4 e). The higher CA is likely a result of increased surface roughness in regional areas of the sand paper treated membrane (Figure 3 j), as the increase of the surface roughness can lead to the enhanced superhydrophobicity.[23] These results suggest that surfaces with wearable superhydrophobicity could be readily obtained by coating the material surface with 3D lipophilic NW networks.

The self-cleaning properties of the membrane were investigated through clearing contaminants, such as dust, off of the membrane. Results show that graphite scrap dust on the membrane can be efficiently removed along the pathway of the rolled water droplet (Figure 4 f). Because of the unique architecture with abundant macropores and superhydrophobic networks in 3D, the NW membrane can act as an absorber for oil/water separation. When a drop of a water/oil (hexane) mixture was applied to the membrane surface, the oil (colored with Oil Red O for visualization) was quickly absorbed by the NW membrane, while the water remained as a droplet on the membrane surface (Figure 4 g). The NW membrane was further applied to clean leaked oil on a water surface. Through dragging the NW membrane around the surface of oil contaminated water (colored with Oil Red O, Figure 4 h), the oil that floated on the water was completely absorbed by the membrane in less than 10 seconds, thus leaving clean water behind in the container (Figure 4 i). The efficiency in oil/water separation can be attributed to the two distinguishing properties of the membrane: high porosity (ca. 80 %) with readily accessible macropores, and 3D superhydrophobic networks. It is envisioned that the hybrid silica NWs and their assemblies can also be used as novel substrates or templates, which provide excellent opportunities in creating new materials with rationally designed properties and functionalities for diverse applications.

In summary, discrete hybrid silica NWs with an average diameter of 80 nm and length up to 12 μm were synthesized by an anisotropic sol-gel growth route. C_{18}TMOS has key roles in controlling the NW diameter below 100 nm and conferring hydrophobicity to the NW surface. The robustness, high colloidal stability, and flexibility of the silica NWs were

exploited to assemble superhydrophobic coatings, free-standing macroporous membranes and monoliths. Access to such NW superstructures provides unprecedented opportunities in developing materials with hierarchical structures and multifunctionalities. Detailed studies on using the silica NWs and their 3D assemblies as substrates or sacrificial templates for preparing multifunctional materials for nanocatalysis, nanosensing, and biomedical applications are currently being explored.

Experimental Section

Preparation of C_{18} alkyl-silica NWs: In a typical synthesis, 1.0 g of polyvinylpyrrolidone (M_w 40 kDa) was dissolved in 10.0 mL of *n*-pentanol in a 15 mL centrifugation tube. Then, 1.0 mL of ethanol, 0.28 mL of deionized water, 0.67 mL of sodium citrate solution (0.18 M in water), and 0.20 mL of ammonia solution (NH_3 content 25 wt%) were added sequentially, and the mixture was shaken by hand for 2 min after each chemical was added. Then, a mixture of 100 μL of TEOS and 10 μL of C_{18}TMOS was added to the above solution and shaken immediately for 5 min. The solution was left static for 24 h at 25 °C. The NWs produced were then separated by centrifugation and washed with ethanol three times, and finally dispersed in ethanol to form a suspension with a silica concentration of 20 mg mL^{-1}.

Silica NW assembly: The dip-coating method was applied to assemble substrate supported NW films. Taking the stainless steel wire mesh substrate as an example, the substrate with dimensions of ca. 1 cm × 1 cm was soaked in the silica NW (with a growth time of 24 h) suspension for 10 s. Following this, the substrate was drawn from the solution and the surplus fluid on the mesh was shaken off by hand and dried in a 100 °C oven for 10 min. The thickness of the silica NW films was adjusted by repeating the dip-coating and drying cycle.

The vacuum filtration method was used to prepare the free-standing NW membranes. In a typical procedure, 10 mL of a diluted NW suspension with a silica concentration of 2 mg mL^{-1} was filtered through a cellulose acetate filter paper (pore size 0.45 μm) to form an interwoven silica NW film on top of the filter paper. After washing with ethanol twice, the silica NW film and filter paper substrate were dried in a 60 °C oven for 30 min. Free-standing silica NW membranes were obtained after being peeled off from the substrate.

Acknowledgments

This work was financially supported by the National Natural Science Foundation of China (21373059), the Australian Research Council (ARC) Centre of Excellence in Convergent Bio-Nano Science and Technology (project number CE140100036), and by the ARC under the Australian Laureate Fellowship (F.C., FL120100030) Scheme. Y.W. acknowledges support from the National 1000 Youth Talents Program of China. X.Z. acknowledges support from an ARC Future Fellowship (FFT120100473).

Keywords: hydrophobic effects · interfaces · membranes · nanostructures · silicates

How to cite: *Angew. Chem. Int. Ed.* **2016**, *55*, 8375–8380
Angew. Chem. **2016**, *128*, 8515–8520

[1] a) A. Stein, B. J. Melde, R. C. Schroden, *Adv. Mater.* **2000**, *12*, 1403–1419; b) Y. Wang, A. Yu, F. Caruso, *Angew. Chem. Int. Ed.* **2005**, *44*, 2888–2892; *Angew. Chem.* **2005**, *117*, 2948–2952; c) F. Hoffmann, M. Cornelius, J. Morell, M. Froba, *Angew. Chem. Int. Ed.* **2006**, *45*, 3216–3251; *Angew. Chem.* **2006**, *118*, 3290–3328; d) J. Chen, X. Wu, X, Hou, X. Su, Q. Chu, N. Fahruddin, J. X. Zhao, *ACS Appl. Mater. Interfaces* **2014**, *6*, 21921–21930; e) Y. Zhang, B. Y. W. Hsu, C. L. Ren, X. Li, J. Wang, *Chem. Soc. Rev.* **2015**, *44*, 315–335; f) V. Malgras, Q. Ji, Y. Kamachi, T. Mori, F. K. Shieh, K. C. W. Wu, K. Ariga, Y. Yamauchi, *Bull. Chem. Soc. Jpn.* **2015**, *88*, 1171–1200; g) N. Song, Y. W. Yang, *Chem. Soc. Rev.* **2015**, *44*, 3474–3504.

[2] a) A. van Blaaderen, R. Ruel, P. Wiltzius, *Nature* **1997**, *385*, 321–324; b) Y. D. Yin, Y. Lu, B. Gates, Y. N. Xia, *J. Am. Chem. Soc.* **2001**, *123*, 8718–8729.

[3] Y. J. Wang, A. K. Wise, J. Tan, J. W. Maina, R. K. Shepherd, F. Caruso, *Small* **2014**, *10*, 4244–4248.

[4] a) A. A. Zakhidov, R. H. Baughman, Z. Iqbal, C. X. Cui, I. Khayrullin, S. O. Dantas, I. Marti, V. G. Ralchenko, *Science* **1998**, *282*, 897–901; b) Y. J. Wang, F. Caruso, *Adv. Funct. Mater.* **2004**, *14*, 1012–1018; c) J. H. Moon, S. Yang, *Chem. Rev.* **2010**, *110*, 547–574; d) J. H. Kim, J. H. Kim, K. H. Choi, H. K. Yu, J. H. Kim, J. S. Lee, S. Y. Lee, *Nano Lett.* **2014**, *14*, 4438–4448.

[5] a) J. W. Liu, H. W. Liang, S. H. Yu, *Chem. Rev.* **2012**, *112*, 4770–4799; b) X. S. Peng, J. Jin, E. M. Ericsson, I. Ichinose, *J. Am. Chem. Soc.* **2007**, *129*, 8625–8633; c) H. W. Liang, L. Wang, P. Y. Chen, H. T. Lin, L. F. Chen, D. He, S. H. Yu, *Adv. Mater.* **2010**, *22*, 4691–4695; d) X. S. Peng, I. Ichinose, *Adv. Funct. Mater.* **2011**, *21*, 2080–2087; e) S. Gong, W. Schwalb, Y. W. Wang, Y. Chen, Y. Tang, J. Si, B. Shirinzadeh, W. L. Cheng, *Nat. Commun.* **2014**, *5*, 3132.

[6] a) Z. W. Pan, Z. R. Dai, C. Ma, Z. L. Wang, *J. Am. Chem. Soc.* **2002**, *124*, 1817–1822; b) E. Murphy-Pérez, S. K. Arya, S. Bhansali, *Analyst* **2011**, *136*, 1686–1689.

[7] Y. F. Shi, *Appl. Phys. Lett.* **2010**, *96*, 121909.

[8] G. Brambilla, D. N. Payne, *Nano. Lett.* **2009**, *9*, 831–835.

[9] Y. L. Hong, X. S. Chen, X. B. Jing, H. S. Fan, B. Guo, Z. W. Gu, X. D. Zhang, *Adv. Mater.* **2010**, *22*, 754–758.

[10] a) B. Platschek, A. Keilbach, T. Bein, *Adv. Mater.* **2011**, *23*, 2395–2412; b) B. Platschek, N. Petkov, D. Himsl, S. Zimdars, Z. Li, R. Kohn, T. Bein, *J. Am. Chem. Soc.* **2008**, *130*, 17362–17371; c) Z. L. Yang, Z. W. Niu, X. Y. Cao, Z. Z. Yang, Y. F. Lu, Z. B. Hu, C. C. Han, *Angew. Chem. Int. Ed.* **2003**, *42*, 4201–4203; *Angew. Chem.* **2003**, *115*, 4333–4335.

[11] a) X. Zhang, F. Shi, J. Niu, Y. G. Jiang, Z. Q. Wang, *J. Mater. Chem.* **2008**, *18*, 621–633; b) K. Yamada, T. G. Henares, K. Suzuki, D. Citterio, *Angew. Chem. Int. Ed.* **2015**, *54*, 5294–5310; *Angew. Chem.* **2015**, *127*, 5384–5401; c) L. P. Wen, Y. Tian, L. Jiang, *Angew. Chem. Int. Ed.* **2015**, *54*, 3387–3399; *Angew. Chem.* **2015**, *127*, 3448–3462.

[12] a) J. H. Zhang, B. Yang, *Adv. Funct. Mater.* **2010**, *20*, 3411–3424; b) J. S. Feng, M. T. Tuominen, J. P. Rothstein, *Adv. Funct. Mater.* **2011**, *21*, 3715–3722; c) J. Y. Shiu, C. W. Kuo, P. L. Chen, C. Y. Mou, *Chem. Mater.* **2004**, *16*, 561–564.

[13] a) L. Jiang, Y. Zhao, J. Zhai, *Angew. Chem. Int. Ed.* **2004**, *43*, 4338–4341; *Angew. Chem.* **2004**, *116*, 4438–4441; b) K. Acatay, E. Simsek, C. Ow-Yang, Y. Z. Menceloglu, *Angew. Chem. Int. Ed.* **2004**, *43*, 5210–5213; *Angew. Chem.* **2004**, *116*, 5322–5325; c) M. L. Ma, M. Gupta, Z. Li, L. Zhai, K. K. Gleason, R. E. Cohen, M. F. Rubner, G. C. Rutledge, *Adv. Mater.* **2007**, *19*, 255–259.

[14] a) C. R. Crick, J. A. Gibbins, I. P. Parkin, *J. Mater. Chem. A* **2013**, *1*, 5943–5948; b) K. K. S. Lau, J. Bico, K. B. K. Teo, M. Chhowalla, G. A. J. Amaratunga, W. I. Milne, G. H. McKinley, K. K. Gleason, *Nano Lett.* **2003**, *3*, 1701–1705; c) J. Yu, L. Qin, Y. F. Hao, S. Kuang, X. D. Bai, Y. M. Chong, W. J. Zhang, E. Wang, *ACS Nano* **2010**, *4*, 414–422.

[15] I. A. Larmour, S. E. J. Bell, G. C. Saunders, *Angew. Chem. Int. Ed.* **2007**, *46*, 1710–1712; *Angew. Chem.* **2007**, *119*, 1740–1742.

[16] a) X. Zhang, F. Shi, X. Yu, H. Liu, Y. Fu, Z. Q. Wang, L. Jiang, X. Y. Li, *J. Am. Chem. Soc.* **2004**, *126*, 3064 – 3065; b) T. Darmanin, E. T. de Givenchy, S. Amigoni, F. Guittard, *Adv. Mater.* **2013**, *25*, 1378 – 1394.
[17] A. Kuijk, A. van Blaaderen, A. Imhof, *J. Am. Chem. Soc.* **2011**, *133*, 2346 – 2349.
[18] Y. S. Sohn, J. Park, G. Yoon, J. Song, S. W. Jee, J. H. Lee, S. Na, T. Kwon, K. Eom, *Nanoscale Res. Lett.* **2010**, *5*, 211 – 216.
[19] G. Poologasundarampillai, B. Yu, J. R. Jones, T. Kasuga, *Soft Matter* **2011**, *7*, 10241 – 10251.
[20] a) Y. Li, G. Zhou, C. Li, D. Qin, W. Qiao, B. Chu, *Colloids Surf. A* **2009**, *341*, 79 – 85; b) T. G. Terentyeva, A. Matras, W. Van Rossom, J. P. Hill, Q. Ji, K. Ariga, *J. Mater. Chem. B* **2013**, *1*, 3248 – 3256; c) Q. Ji, C. Guo, X. Yu, C. J. Ochs, J. P. Hill, F. Caruso, H. Nakazawa, K. Ariga, *Small* **2012**, *8*, 2345 – 2349.
[21] L. Alibardi, D. P. Edward, L. Patil, R. Bouhenni, A. Dhinojwala, P. H. Niewiarowski, *J. Morphol.* **2011**, *272*, 758 – 768.
[22] L. Feng, S. H. Li, H. J. Li, J. Zhai, Y. L. Song, L. Jiang, D. B. Zhu, *Angew. Chem. Int. Ed.* **2002**, *41*, 1221 – 1223; *Angew. Chem.* **2002**, *114*, 1269 – 1271.
[23] F. J. Wang, S. Yu, J. F. Ou, M. S. Xue, W. Li, *J. Appl. Phys.* **2013**, *114*, 124902.

Received: April 14, 2016
Revised: May 5, 2016
Published online: June 9, 2016

